ISSN(Online): 2319-8753
ISSN (Print): 2347-6710

International Journal of Innovative Research in Science, Engineering and Technology

(An ISO 3297: 2007 Certified Organization)

Website: www.ijirset.com

Vol. 6, Issue 5, May 2017

# Numerical and Experimental Study of Temperature Distribution in Friction Stir Spot Welding of AA2024-T3 Aluminum Alloy

Abdul Wahab H. Khuder[1], Muhammed A. Muhammed[2], Haidar K. Ibrahim[3]

Asst. Professor, Engineering Technical College-Baghdad, Middle Technical University, Baghdad, Iraq[1]

Asst. Professor, Mechanical Engineering Department, College of Engineering, Nahrain University, Baghdad, Iraq[2]

M.Tec Student, Welding Engineering Department, Engineering Technical College-Baghdad, Middle Technical University, Baghdad, Iraq[3]

**Abstract**: Friction stir spot welding (FSSW) is a type of solid state joining processes, which was derived from the linear friction stir welding (FSW) as an alternative method for single-point joining processes like resistance spot welding and fastening. Two types of tool pin geometry (straight cylindrical & triangular) and constant tool rotational speed of (535 rpm) were used to evaluate the temperature distribution during welding process. Two thermocouples (K-type) were used at the center of weld nugget and at a distance of 7mm from the center of the spot to measure the temperature distribution experimentally. The three dimensional non-linear numerical model using ANSYS 15.0 was built to simulate temperature distribution during FSSW process with the cylindrical and triangular tool pin profiles. The peak temperature obtained was 50% of the melting point of base material. A good agreement was obtained between ANSYS model results and those recorded experimentally during FSSW process.

**Keywords**: AA2024-T3 Al alloy, Friction stir spot welding, Temperature distribution, Weld nugget, ANSYS model.

## I. INTRODUCTION

The highly alloyed 2XXX series (aluminum-copper alloys) are used extensively in aerospace industries which need to produce high strength fatigue and fracture resistance joints. These aluminum alloys are generally classified as non-weldable alloys [1]. One of the challenges in the fusion welding of these alloys is their high susceptibility to hot cracking during solidification. In addition, the decreasing in mechanical properties causes by dissolution of strengthening precipitates during fusion welding [2]. Friction stir welding (FSW) is a solid state welding process that was invented by Wayne Thomas at The Welding Institute (TWI), United Kingdom, in 1991 [3], and has emerged as a welding technique used in high strength alloys (2XXX, 6XXX, and 7XXX series) for aerospace, automotive and marine applications [4]. During FSW, the maximum temperature of the welded plates is typically ranges from 70% to 90% of the melting temperature of the workpiece material [5], so that better mechanical properties and fewer weld defects of the weld zone are produced when compared with conventional fusion welding [6,7,8]. Based on friction stir welding (FSW), the Mazda Corporation of Japan proposed a friction stir spot welding (FSSW) method in an attempt to transfer some of the advantages of FSW to spot welding [9]. The FSSW can also be called as conventional FSSW, which has been firstly applied in the real production line for Mazda RX-8 hood and rear door panel in 2003 [10,11]. Friction stir spot welding (FSSW) consists of three phases: plunging, stirring, and retracting as shown in Figure 1. A non-consumable rotating tool is plunged into the overlapped workpieces that to be joined, held for a certain duration time (dwell time) and finally it retracted from the workpiece with no lateral movement or translation. The frictional heat generated at the tool-workpiece interface softens the surrounding materials. The rotational action and the downward force of the tool causes the material flow and mixing of the plasticized materials of upper and lower sheets result in the formation of a solid-state weld region [12,13,14].

ISSN(Online): 2319-8753
ISSN (Print): 2347-6710

International Journal of Innovative Research in Science, Engineering and Technology

(An ISO 3297: 2007 Certified Organization)

Website: www.ijirset.com

Vol. 6, Issue 5, May 2017

Objective of this work is to predict numerical transient temperature distribution in AA2024-T3 sheets that were welded by FSSW, and compare the results obtained from the thermal analysis with those measured experimentally during the welding process.

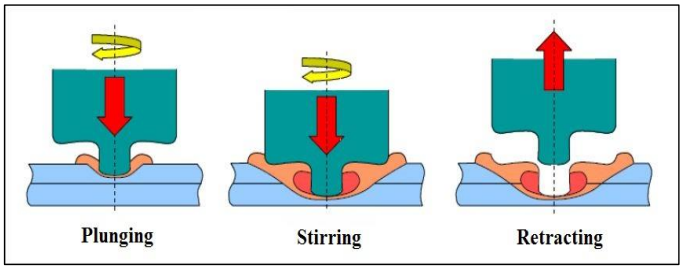


Figure 1: Schematic illustration of conventional FSSW process [12].

## II. MATERIALS AND METHODS

AA2024-T3 aluminum alloy, with 2mm sheets thickness, were chosen as the base material. The chemical composition and mechanical properties are listed in tables (1, and 2), respectively. The temperature-dependent properties of AA2024-T3 aluminum alloy at various temperatures are given in table 3 [15, 16].

Table 1: Chemical composition of AA2024 aluminum alloy sheets (wt %).

| Si | Fe | Cu | Mn | Mg | Cr | Ni | Zn | Ti | V | Ga | Al |
|---|---|---|---|---|---|---|---|---|---|---|---|
| 0.103 | 0.197 | 4.84 | 0.645 | 1.5 | 0.027 | 0.006 | 0.181 | 0.042 | 0.017 | 0.016 | Bal. |

Table 2: Mechanical properties of AA2024-T3 aluminum alloy used in this work.

| Tensile Strength (MPa) | Yield Strength (MPa) | Elongation (%) |
|---|---|---|
| 486 | 360 | 20 |

Table 3: Temperature dependent material properties of AA2024-T3 [15, 16].

| Temperature (℃) | Thermal Conductivity ($w.m^{-1}.K^{-1}$) | Specific Heat ($J.Kg^{-1}.K^{-1}$) | Elastic Modulus (GPa) | Poison's Ratio | Yield Strength (MPa) | Density ($Kg.m^{-3}$) | Thermal Expansion/ $10^{-6}$ |
|---|---|---|---|---|---|---|---|
| 20 | 164 | 881 | 72.4 | 0.33 | 473 | 2780 | 14 |
| 100 | 182 | 927 | 66.5 | 0.33 | 416.5 | 2780 | 23.018 |
| 200 | 194 | 1047 | 63.5 | 0.33 | 293.5 | 2780 | 24.509 |
| 300 | 202 | 1130 | 60.4 | 0.33 | 239.5 | 2780 | 25.119 |
| 400 | 210 | 1210 | 56.1 | 0.33 | 150 | 2780 | 25.594 |
| 500 | 220 | 1300 | 50 | 0.33 | 100 | 2780 | 26.637 |

The FSSW tools fabricated from tool steel AISI D3 (labeled as X210Cr12) with hardness of 58HRC. The chemical composition of the tools material is listed in table 4. Two different tools were used in this work. They have cylindrical and triangular tool pin profiles; each one of them consists of a flat shoulder with diameter of 18mm. The diameter of the cylindrical pin and the circle diameter, which is the circumference of the triangular pin, were 5 mm, respectively, as shown in figure 2.

Table 4: Chemical composition of tool steel X210Cr12 used in this work (wt %).

| C | Mn | P | S | Si | Cr | V | Mo |
|---|---|---|---|---|---|---|---|
| 2.11 | 0.35 | 0.06 | 0.02 | 0.21 | 12 | 0.11 | 0.17 |

ISSN(Online): 2319-8753
ISSN (Print): 2347-6710

International Journal of Innovative Research in Science, Engineering and Technology

(An ISO 3297: 2007 Certified Organization)

Website: www.ijirset.com

Vol. 6, Issue 5, May 2017

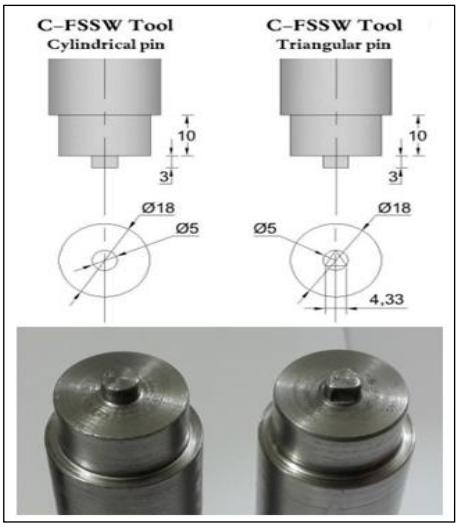


Figure 2: Shapes and dimensions of the FSSW tools used in this work (All dimensions in mm).

To achieve a FSSW joint, the rotating tool plunged 0.4mm with manual feed at a constant rate of 0.47mm/min for a specified time 2 sec (dwell time) at a rotational speed of (535rpm). The plunging depth that resulted from tool penetration was approximately 85% of the total sheet thickness.

Thermal cycles and temperature distribution in the weld area were measured during FSSW process. Two thermocouples type K (-100℃ to 1100℃) were positioned in two locations within the welded area, as schematically shown in figure 3, to obtain different readings of the temperature experimentally at that locations. One of the thermocouples (T1) was welded at the center of nugget zone (NZ) on the bottom surface of the lower sheet, and the other thermocouple (T2) was inserted at a distance of 7mm from the center of NZ using an internal groove created on the top surface of the lower sheet in order to pass thermocouple wire through it to the desired location. Figure 4(a) shows thermocouple locations on the workpiece before conduct the FSSW process. Thermocouples were connected to the digital readers used to display the measured temperature, see figure 4(b).

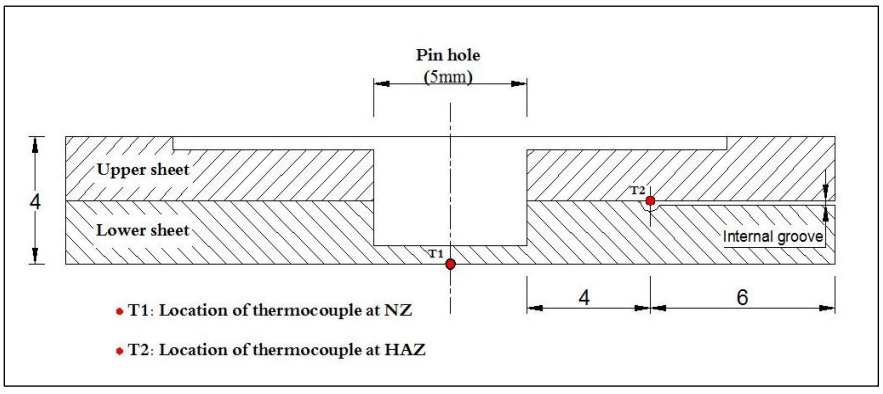


Figure 3: A schematic cross-section shows thermocouples sites.

ISSN(Online): 2319-8753
ISSN (Print): 2347-6710

International Journal of Innovative Research in Science, Engineering and Technology

(An ISO 3297: 2007 Certified Organization)

Website: www.ijirset.com

Vol. 6, Issue 5, May 2017

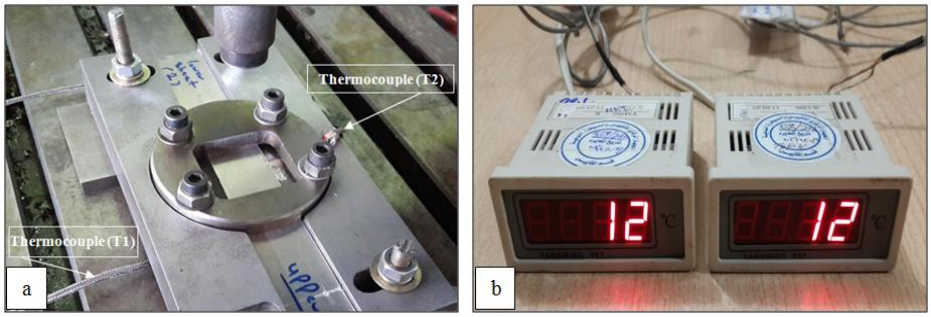


(a) (b)

Figure 4: (a) Thermocouple locations on the workpiece before conducting FSSW process, (b) digital readers.

Two cases are considered with different tool pin profiles (cylindrical and triangular) under constant tool rotational speed of 535rpm for measuring the axial load during the FSSW process for dwell time (2sec). A component dynamometer based on load cell (SEWHA, 2000kg capacity, R.O:2.002mV/V) was fixed on a special rig designed for this purpose, see figure 5. Weight indicator (SEWHA, SI4010) was used for display the analogue force data which are transmitted from the load cell.


Figure 5: Axial load measuring rig.

## III. FINITE ELEMENT MODEL

A multi-purpose finite element program ANSYS®15.0 was used for numerical simulation of the temperature distribution during friction stir spot welding process. A three dimensional transient, nonlinear heat transfer model was developed to determine the temperature fields.

### Thermal Model

Thermal model is used for the purpose of calculate the transient temperature fields that developed in the weld area during the FSSW process. The transient temperature field is a function with the time and spatial coordinates (x, y, z), are estimated by the three dimensional nonlinear heat transfer equation:

$$k(T)\left(\frac{\partial^2 T}{\partial x^2}+\frac{\partial^2 T}{\partial y^2}+\frac{\partial^2 T}{\partial z^2}\right)+Q_{int}=C(T)\rho(T)\frac{\partial T}{\partial t} \quad \ldots\ldots\ldots \text{equation (1)}$$

where T is the absolute temperature, t is the time, k is a coefficient of thermal conductivity along x, y, z directions, $Q_{int}$ is the internal heat source rates in the three axis, C is a specific heat of workpiece, and $\rho$ is temperature dependent density of the workpiece [15, 17].

ISSN(Online): 2319-8753
ISSN (Print): 2347-6710

International Journal of Innovative Research in Science, Engineering and Technology

(An ISO 3297: 2007 Certified Organization)

Website: www.ijirset.com

Vol. 6, Issue 5, May 2017

**Assumptions**

Several simplifying assumptions have been made in developing the FEM thermal model:

- Workpiece material is isotropic and homogenous.
- No melting occurs during FSSW process.
- Heat transfer from the workpiece to the workpiece fixture is negligible.
- Initial temperature is assumed to be 25℃ .
- It is assumed that 100% of the dissipated energy caused by friction is transformed into heat.
- The tool and workpiece fixture are assumed rigid and no deformation occurs in these parts.

**Boundary Conditions**

Boundary conditions for FSSW thermal model were applied as surface loads through ANSYS program. Assumptions were made for various boundary conditions based on data collected from various published papers [18,19,20]. Convection and radiative heat losses to the ambient take place across all free surfaces of the workpiece, while conduction losses occur from the upper and bottom surfaces of the workpiece to the workpiece fixture. To account the convection and radiation effects on all free surfaces of the welded sheets, the heat loss ($q_s$) is calculated by equation (2).

$$q_s = \beta\,(T - T_o) + \eta\,\xi\,\varepsilon\,(T^4 - T_o^4) \quad \text{..... equation (2)}$$

where T is the absolute temperature of the workpiece surfaces, $T_o$ is the absolute temperature of the ambient, $\beta$ is the convection heat transfer coefficient, ε is the emissivity of the workpiece surfaces, η is the radiation factor, and ξ is the Stefan-Boltzmann constant ($5.67\times10^{-12}$ W/cm$^2$.℃). In the current model, the typical values of $\beta$, ε, and η were taken to be 30 w/m$^2$ °C, 0.5, and 1 for aluminum, respectively, with an ambient temperature ($T_o$) of 300°K. In order to account for the conductive heat loss through the bottom and upper surfaces of weld sheets, a high overall heat transfer coefficient was assumed based on previous study [21]. The heat loss was modelled approximately using heat flux loss by convection $q_b$ , which given by equation (3).

$$q_b = \beta_b\,(T - T_o) \quad \text{..... equation (3)}$$

where $\beta_b$ is a fictitious convection coefficient. In the present study, the optimized value of , between the workpiece and the fixture, was taken to be 418 w/m$^2$ k [22].

Heat generation during FSSW arises from three heat sources: friction work at the tool shoulder and upper sheet interface, friction work at the upper and lower sheet interface, and plastic deformation of the material around the tool pin [23]. A previous study [19] showed that the heat generated due to the friction work at the interface of the tool and the upper sheet contributes the most heat to the welding process, which is about 96.84% of the total heat generated from FSSW, while the rest of the heat energies come from the friction force at the interface between the overlapped sheets (0.02%), and the plastic deformation in the material (3.14%). Thus, the heat generation is assumed occur predominantly under the tool shoulder as a main heat source, and the other sources were almost negligible.

Frictional heat for the rotating tool at rubbing angular speed of (1- $\delta$) $\omega$ is:

$$dQ = (1-\delta)\,\omega\,dM = 2\pi\,(1-\delta)\,\omega\,\mu\,P\,r^2\,dr \quad \text{..... equation (4)}$$

where δ is the slip factor that compensates for tool/material relative velocity. Typical values for slip factor were found in the ranges of 0.6 – 0.85 [24].

Frictional heat of tool shoulder will be:

$$Q_{shoulder} = \int_0^R dQ = \frac{2}{3}\,\pi\,(1-\delta)\,\omega\,\mu\,P\,R_s^3 \quad \text{..... equation (5)}$$

In similar concept, heat generated by lateral surface of the tool pin is:

$$Q_{pin} = 2\pi\,(1-\delta)\,\omega\,\mu\,P\,L_p\,R_p^2 \quad \text{..... equation (6)}$$

The temperature gradient in two points, which are located at similar positions of thermocouples T1 and T2, was calculated to compare these data with that measured experimentally to validate the results. Heat transfer coefficient is 300w/m$^2$ k, convection heat transfer coefficient is 30w/m$^2$ k [21, 22], ambient temperature $T_o$= 300°k, slip factor $\delta$= 0.8 [25], and friction coefficient $\mu$= 0.4 [17]. The heat generation (Q) was calculated from equations (5) & (6) based upon the coefficient of friction ($\mu$), pressure (P) in addition to other welding parameters such as the tool rotational speed and tool pin geometries. The value of pressure (P) was calculated from dividing the axial load by the contact surface area. Then, the heat calculated (Q) was used as input load to ANSYS model. In order to evaluate temperature distribution during welding process, the frictional heat was simulated by change the heat source location (FSSW tool) depending on the overall welding time and tool plunging depths.

ISSN(Online): 2319-8753
ISSN (Print): 2347-6710

International Journal of Innovative Research in Science, Engineering and Technology

(An ISO 3297: 2007 Certified Organization)

Website: www.ijirset.com

Vol. 6, Issue 5, May 2017

## IV. RESULTS AND DISCUSSION

During FSSW process, temperature rises when the rotating pin penetrates the upper sheet through plunging of FSSW tool into the workpiece. After that, temperature increases at a rapid rate when the shoulder makes contact with the upper surface of the workpiece. At the final stage, tool is retracted and the welded joint is cooled to the room temperature. Figure 6(a, and b) show the measured temperature profiles for the complete welding cycle during FSSW using the cylindrical and triangular tool pin shapes, respectively.

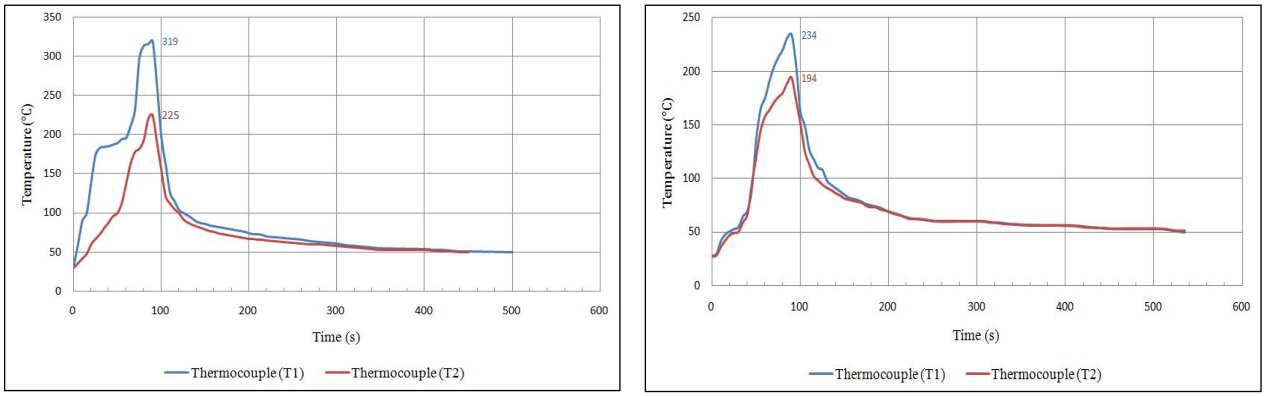


(a) (b)

Figure 6: Experimental temperature profiles for FSSW process using different tool pin profiles, (a) cylindrical pin, and (b) triangular pin

As evident in the above figures, temperature profile of thermocouple (T1) is higher than that of thermocouple (T2) in both cases. For the cylindrical pin-welds, the maximum temperature measured by thermocouple T1 is (319℃), while the maximum temperature of thermocouple T2 is (225℃). Also, for the triangular pin-welds, the peak temperature measured from thermocouple T1 is (234℃), while the peak temperature from T2 is (194℃). This difference in thermocouple readings between T1 and T2 may be attributed to variation of heat generated in the FSSW regions during welding process. The nugget zone (NZ) is subjected to severe plastic deformation for welding materials caused by rotation of the tool pin, in addition to the frictional heat generated between the deformed materials and the pin surfaces, which causes an increase in temperature of this region as compared with the other welding zones. While the region located at a distance of 7mm (T2) is only exposed to frictional heating resulting from rotation of the tool shoulder [26], so the temperature profile of thermocouple (T2) is lower than that of thermocouple at center of the spot (T1).

It is clear from the above figures that the temperature profile of the cylindrical pin is higher than that of the triangular pin. This is because the cylindrical pin has a larger surface projected area at the pin tip than the tip surface of the triangular pin, see figure 7, which causes more frictional heat at periphery of the cylindrical pin as a result of the large frictional area between the lateral surfaces of the pin and the welding material [27].

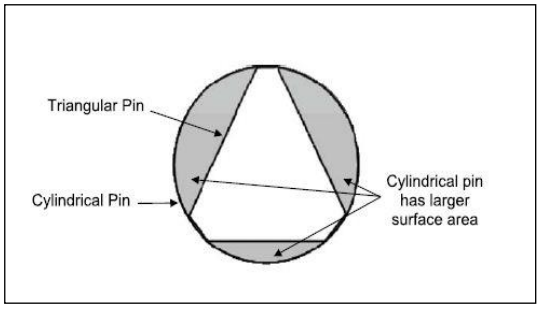


Figure 7: A sketch for comparison between the frontal area of the cylindrical and triangular tool pin profiles [28].

ISSN(Online): 2319-8753
ISSN (Print): 2347-6710

International Journal of Innovative Research in Science, Engineering and Technology

(An ISO 3297: 2007 Certified Organization)

Website: www.ijirset.com

Vol. 6, Issue 5, May 2017

Depending on the overall welding time (90 sec) and tool plunging depth (3.4mm), the heat source location (tool plunging depth) was divided into four steps of (0.85, 1.7, 2.55 and 3.4mm) during four welding times of 22.5 sec, 45 sec, 67.5 sec, and 90 sec, respectively. Tables (5 & 6) present the calculated heat generation (Q) during FSSW using the cylindrical and triangular tool pin profiles, respectively.

Table 5: Frictional heat applied by the rotating tool with a cylindrical pin.

| Plunging Depth (mm) | | Axial Load (N) | Pressure (MPa) | Q (Watt) |
|---|---|---|---|---|
| 0.85 | | 2980 | 151.77 | 22.7 |
| 1.7 | | 2435 | 124 | 37.1 |
| 2.55 | | 2285 | 116.37 | 52.2 |
| 3.4 | Pin | 450 | 22.92 | 12.1 |
| | Shoulder | 5500 | 23.42 | 156.8 |

Table 6: Frictional heat applied by the rotating tool with a triangular pin.

| Plunging Depth (mm) | | Axial Load (N) | Pressure (MPa) | Q (Watt) |
|---|---|---|---|---|
| 0.85 | | 1520 | 129.36 | 19.35 |
| 1.7 | | 770 | 65.53 | 19.6 |
| 2.55 | | 845 | 71.91 | 32.28 |
| 3.4 | Pin | 240 | 20.42 | 10.78 |
| | Shoulder | 5100 | 21 | 140.7 |

Figures (8 and 9) show the isometric views of the workpieces at different friction stir spot welding times using the cylindrical and triangular tool pin profiles, respectively. As shown from these figures, the workpiece welded using the cylindrical pin had higher temperature distribution than that welded by the triangular pin. This is because the frictional area of the cylindrical pin is higher than that of the triangular pin, as illustrated previously in figure 7. The highest temperature was observed at the center of weld nugget, because the rotation of the tool pin and shoulder contribute to the highest heat flux in this region.

ISSN(Online): 2319-8753
ISSN (Print): 2347-6710

International Journal of Innovative Research in Science, Engineering and Technology

(An ISO 3297: 2007 Certified Organization)

Website: www.ijirset.com

Vol. 6, Issue 5, May 2017

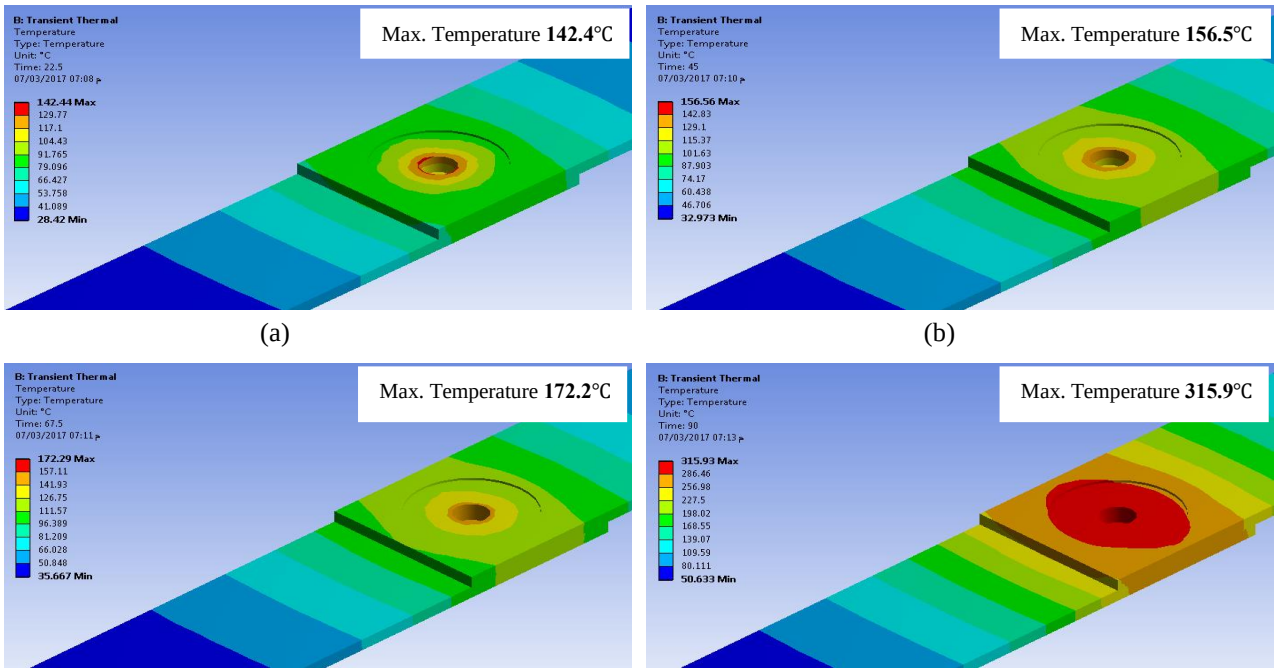


Figure 8: Isometric view of temperature distribution for different welding times in FSSW joint welded by the cylindrical tool pin profile, (a) 22.5sec, (b) 45sec, (c) 67.5sec, and (d) 90 sec

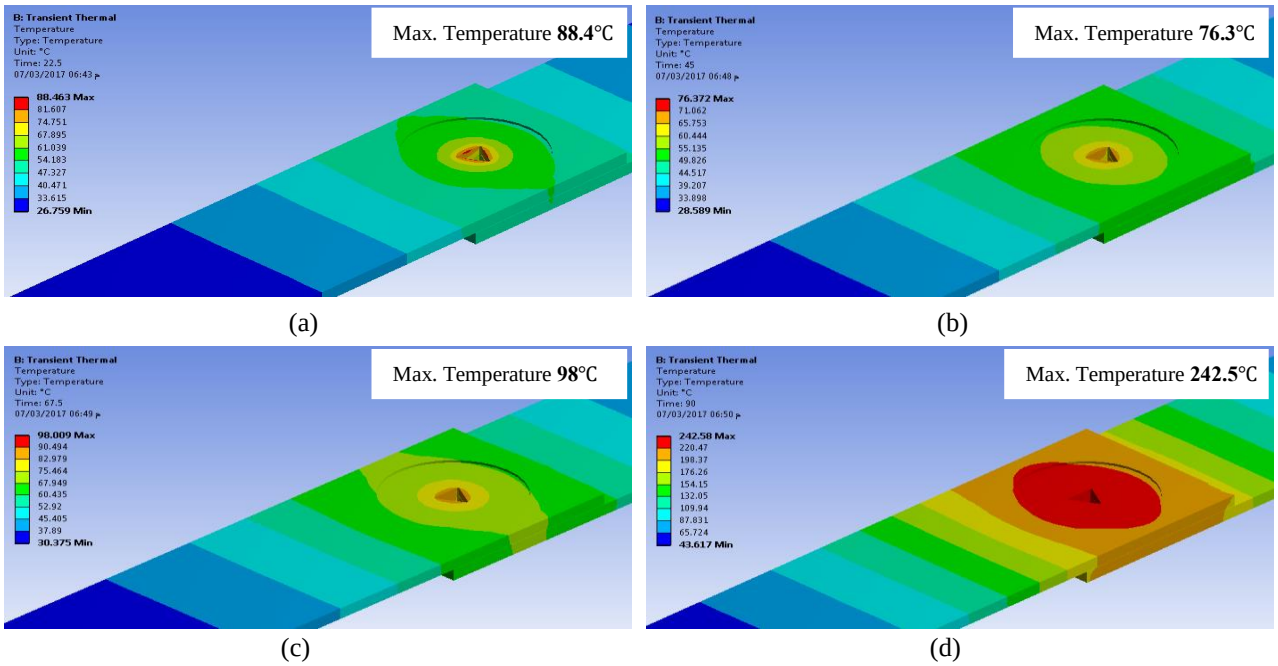


Figure 9: Isometric view of temperature distribution for different welding times in FSSW joint welded by the triangular tool pin profile, (a) 22.5sec, (b) 45sec, (c) 67.5sec, and (d) 90 sec

ISSN(Online): 2319-8753
ISSN (Print): 2347-6710

International Journal of Innovative Research in Science, Engineering and Technology

(An ISO 3297: 2007 Certified Organization)

Website: www.ijirset.com

Vol. 6, Issue 5, May 2017

Figures (10 – 11) show a comparison of the temperature distribution measured experimentally and those calculated by ANSYS model. Figure 10 (a and b) show the temperature distribution profiles which are obtained from the tested regions at center of the weld nugget and at a distance of 7mm from the center of the spot, respectively. At the center of weld nugget, the maximum temperature measured experimentally in welds using the cylindrical pin was (319℃) while with ANSYS model, it was found to be (315℃). Also, at the same time, the maximum temperature obtained at 7mm from the spot center was (225℃) and (255℃) in the experimental and ANSYS model results, respectively. On the other hand, the maximum temperature obtained at center of the spot in the welds using the triangular pin was (234℃) and (242℃) in the experimental and ANSYS model results, respectively, as shown in figure 11(a). While, at a distance of 7mm, the maximum temperature obtained for both experimental and ANSYS model results was (194℃) and (210℃), respectively, during FSSW process using the triangular pin, as shown in figure 11(b). Table 7 summarizes maximum temperatures measured during the experimental tests and those calculated using ANSYS model at different test regions.

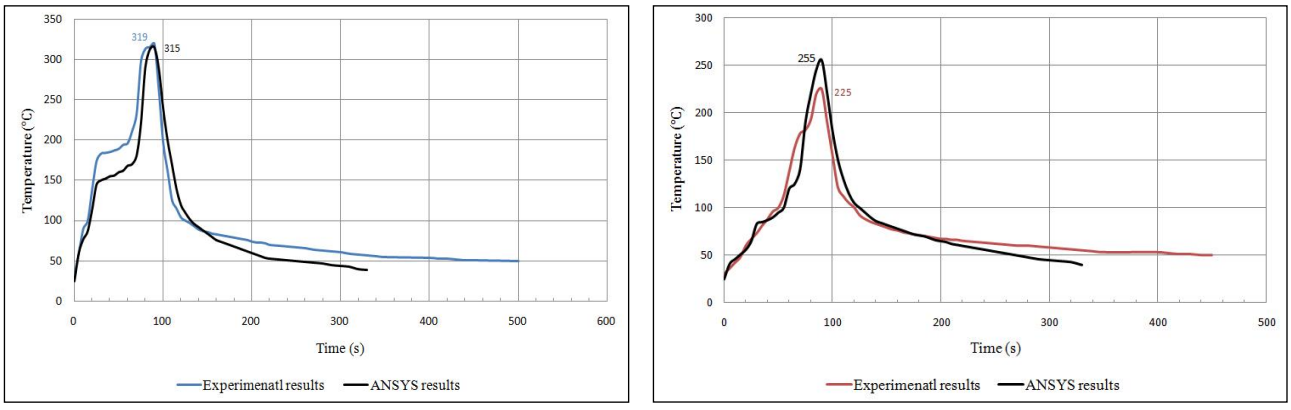


(a) (b)

Figure 10: Comparison of the experimental and ANSYS model results obtained at different tested regions during FSSW using the cylindrical tool pin profile, (a) at the center of weld nugget (T1 location), (b) at a distance of 7mm from the center of the spot (T2 location)

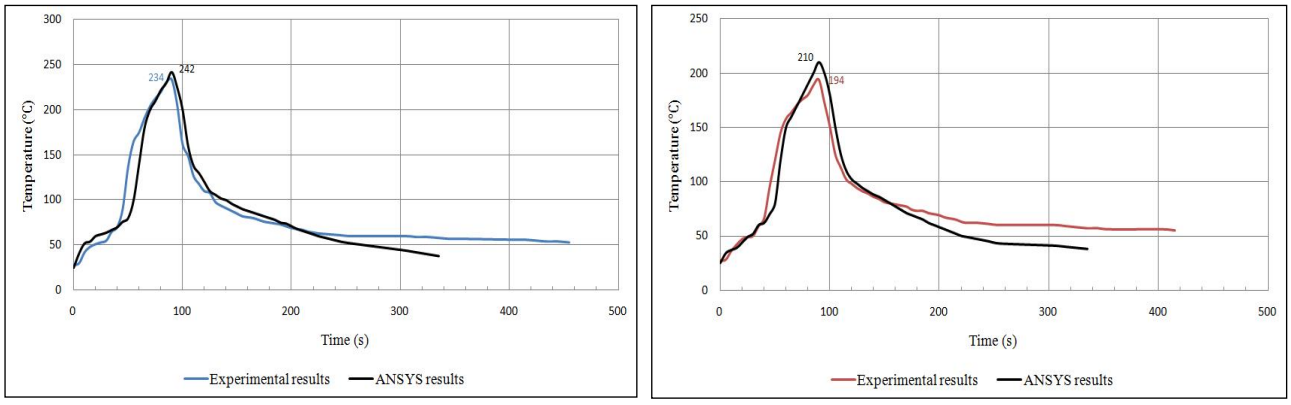


(a) (b)

Figure 11: Comparison of the experimental and ANSYS model results obtained at different tested regions during FSSW using the triangular tool pin profile, (a) at the center of weld nugget (T1 location), (b) at a distance of 7mm from the center of the spot (T2 location)

ISSN(Online): 2319-8753
ISSN (Print): 2347-6710

International Journal of Innovative Research in Science, Engineering and Technology

(An ISO 3297: 2007 Certified Organization)

Website: www.ijirset.com

Vol. 6, Issue 5, May 2017

Table 7: Maximum temperatures obtained from the experimental tests and ANSYS model during FSSW process using different tool pin profiles

| Tool Pin Profile | Tested Region | Experimental Test Results | ANSYS Model Results | Error (%) |
|---|---|---|---|---|
| Cylindrical | At the center of the spot | 319 | 315 | 1.25 |
| | At a distance of 7mm from the center of the spot | 225 | 255 | 11.76 |
| Triangular | At the center of the spot | 234 | 242 | 3.3 |
| | At a distance of 7mm from the center of the spot | 194 | 210 | 7.62 |

From the above results, it can be observed that the discrepancy between the experimental test and ANSYS model results in maximum temperature was (1.25% - 11.76%) at different test regions during FSSW with different tool pin profiles. Also, it can be seen that the trend of the temperature profiles between the experimental and ANSYS model results was almost identical. This indicates that the variable inputs and the assumptions adopted in ANSYS model were reasonable.

## V. CONCLUSIONS

In this paper, a systematic numerical analysis using ANSYS-software and experimental temperature distribution using thermocouples in friction stir spot welded 2mm sheets of AA2024-T3 allow several conclusions to be drawn.

1. Axial load of the rotating tool significantly affected by the tool pin profile at a constant plunging speed (0.47mm/min). The axial load obtained from the cylindrical pin during FSSW process is higher compared with that obtained by the triangular pin at the same conditions.
2. Temperature distribution during FSSW directly affected by the tool pin geometry at a constant tool rotational speed (535rpm). The maximum temperature measured at center of the spot during welding process using the cylindrical and triangular tool pin profiles is 319℃ and 234℃, respectively.
3. The maximum temperature measured during FSSW using the cylindrical tool pin profile is 319℃, which is (50%) less than the liquidus temperature of the base material AA2024-T3 (638℃).
4. At the center of the spot weld, a good agreement obtained between the maximum temperatures measured experimentally and those obtained numerically from the simulation results during FSSW process with discrepancy of (1.25 – 3.3) %.

## REFERENCES

[1] R. Mishra and Z. Ma, "Friction stir welding and processing", Materials Science and Engineering R, Vol.50, pp.1-78, August 2005.
[2] V. Jalilvand, H. Omidvar and H. Khorrami, "Effect of welding parameters on the mechanical properties of AA2024 aluminium alloy joints welded by resistance seam welding", Canadian Metallurgical Quarterly, Vol.53, Issue 2, 2014.
[3] S. P. Pawar and M. T. Shete, "OPTIMIZATION OF FRICTION STIR WELDING PROCESS PARAMETER USING TAGUCHI METHOD AND RESPONSE SURFACE METHODOLOGY: A REVIEW", International Journal of Research in Engineering and Technology, Vol.2, Issue 12, pp.551-554, December 2013.
[4] H. S. Patil and S. N. Soman, "Experimental study on the effect of welding speed and tool pin profiles on AA6082-O aluminium friction stir welded butt joints", International Journal of Engineering, Science and Technology, Vol.2, Issue 5, pp.268-275, 2010.
[5] M. Jweeg, M. Tolephih, M. Muhammed and G. Sadiq, "Numerical and experimental analysis of transient temperature and residual thermal stresses in friction stir welding of aluminum alloy 7020-T53", ARPN Journal of Engineering and Applied Sciences, Vol.11, Issue 19, October 2016.
[6] S. A. Khodir and T. Shibayanagi, "Microstructure and Mechanical Properties of Friction Stir Welded Dissimilar Aluminum Joints of AA2024-T3 and AA7075-T6", Materials Transactions, Vol.48, Issue7, pp.1928-1937, 2007.
[7] P. Prasanna, C. Penchalayya and D. Rao, "Optimization and Validation of Process Parameters in Friction Stir Welding on AA 6061 Aluminum Alloy Using Gray Relational Analysis", International Journal of Engineering Research and Applications (IJERA), Vol.3, Issue 1, pp.1471-1481, 2013.
[8] A. S. Gupta and S. P. Patel, "Experimental Evaluation on the Effect of Welding Speed and Tool Pin Profiles on Friction Stir Welded Joints on AA 6082-T6", International Journal of Engineering Research & Technology (IJERT), Vol.3, Issue 5, pp.2257-2262, 2014.

ISSN(Online): 2319-8753
ISSN (Print): 2347-6710

International Journal of Innovative Research in Science, Engineering and Technology

*(An ISO 3297: 2007 Certified Organization)*

*Website: www.ijirset.com*

**Vol. 6, Issue 5, May 2017**

[9] T. Iwashita, "METHOD AND APPARATUS FOR JOINING", U.S. Patent 6,601,751 B2, August 2003.
[10] Mazda media release, "Mazda Develops World's First Steel and Aluminum Joining Technology Using Friction Heat", Products and Technology, 2005.
[11] J. Piccini and H. Svoboda, "Effect of pin length on Friction Stir Spot Welding (FSSW) of dissimilar Aluminum-Steel joints", Procedia Materials Science, Vol.9, pp.504-513, 2015.
[12] H. Ibrahim, A. Khuder and M. Muhammed, "Effects of Rotational Speeds and Tool Pin Geometry on Microstructure and Mechanical Properties of Refilled Friction Stir Spot Welds of Similar AA2024-T3 Aluminum Alloy Sheets", International Journal of Engineering Research & Technology (IJERT), Vol.6, Issue 04, pp.937-952, April-2017.
[13] Y. Bozkurt and M. Bilici, "Taguchi Optimization of Process Parameters in Friction Stir Spot Welding of AA5754 and AA2024 Alloys", Advanced Materials Research, Vol.1016, pp.161-166, 2014.
[14] M. Bilici, "Effect of tool geometry on friction stir spot welding of polypropylene sheets", eXPRESS Polymer Letters, Vol.6, Issue 10, pp.805-813, 2012.
[15] K. Salloomi, L. Sabri, Y. Hamad and S. Mohammed, "3-Dimensional Nonlinear Finite Element Analysis of both Thermal and Mechanical Response of Friction Stir Welded 2024-T3 Aluminum Plates", Journal of Information Engineering and Applications, Vol.3, Issue 9, 2013.
[16] N. Zhao, Y. Yang, M. Han, X. Luo, G. Feng and R. Zhang, "Finite element analysis of pressure on 2024 aluminum alloy created during restricting expansion-deformation heat-treatment", Transactions of Nonferrous Metals Society of China, Vol.22, pp.2226-2232, 2012.
[17] S. Hussein, S. Thiru, R. Izamshah and A. Tahir, "Unstable Temperature Distribution in Friction Stir Welding", Advances in Materials Science and Engineering, Vol.2014, Issue ID 980636, pp.1-8, 2014.
[18] Q. Doos, M. Jweeg and S. Ridha, "Analysis of Friction Stir Welds. Part I: Transient Thermal Simulation Using Moving Heat Source", The 1st Regional Conference of Engineering and Science NUCEJ, Vol.11, Issue 3, pp.429-437, 2008.
[19] M. Awang and V. Mucino, "Energy Generation during Friction Stir Spot Welding (FSSW) of Al 6061-T6 Plates", Materials and Manufacturing Processes, Vol.25, Issue 1-3, pp.167-174, 2010.
[20] A. Takhakh and H. Shakir, "Experimental and numerical evaluation of friction stirs welding of AA2024-W aluminum alloy", Journal of Engineering, Vol.18, Issue 6, 2012.
[21] M. Malde, "Thermomechanical modeling and optimization of friction stir welding", M.Sc. thesis, Department of Construction Management and Industrial Engineering, Agricultural and Mechanical College, Louisiana State University, December 2009.
[22] R. Nandan, G. Roy, T. Lienert and T. DebRoy, "Numerical modelling of 3D plastic flow and heat transfer during friction stir welding of stainless steel", Science and Technology of Welding and Joining, Vol.11, Issue 5, pp.526-537, 2006.
[23] M. Awang, "Simulation of Friction Stir Spot Welding (FSSW) Process: Study of Friction Phenomena", Ph.D. dissertation, Department of Mechanical and Aerospace Engineering, West Virginia University, 2007.
[24] J. Dixon, D. Burkes and P. Medvedev, "Thermal Modeling of a Friction Bonding Process", Proceedings of the COMSOL Conference, October 2007.
[25] M. Jweeg, M. Tolephih and M. Muhammed, "Effect of friction stir welding parameters (rotation and transverse) speed on the transient temperature distribution in friction stir welding of AA 7020-T53", ARPN Journal of Engineering and Applied Sciences, Vol.7, Issue 4, 2012.
[26] V. Patel, D. Sejani, N. Patel, J. Vora, B. Gadhvi, N. Padodara and C. Vamja, "Effect of Tool Rotation Speed on Friction Stir Spot Welded AA5052-H32 and AA6082-T6 Dissimilar Aluminum Alloys", Metallography, Microstructure, and Analysis, Vol.5, Issue 2, pp.142-148, 2016.
[27] Q. Atiah, S. Al-Rubaii and Z. Al-Tahir, "Determination of Optimum Tool Design for FSW AA2024-T351", Engineering & Technology Journal, Vol.32 Part (A), Issue 11, 2014.
[28] H. Badarinarayan, Y. Shi, X. Li and K. Okamoto, "Effect of tool geometry on hook formation and static strength of friction stir spot welded aluminum 5754-O sheets", International Journal of Machine Tools and Manufacture, Vol.49, Issue 11, pp.814-823, 2009.